JACS
JOURNAL OF THE AMERICAN CHEMICAL SOCIETY

Communication

pubs.acs.org/JACS

Label-Free SERS Monitoring of Chemical Reactions Catalyzed by Small Gold Nanoparticles Using 3D Plasmonic Superstructures

Wei Xie, Bernd Walkenfort, and Sebastian Schlücker*

Department of Physics, University of Osnabrück, Barbarastrasse 7, 49076 Osnabrück, Germany

Supporting Information

ABSTRACT: Label-free in situ surface-enhanced Raman scattering (SERS) monitoring of reactions catalyzed by small gold nanoparticles using rationally designed plasmonic superstructures is presented. Catalytic and SERS activities are integrated into a single bifunctional 3D superstructure comprising small gold satellites self-assembled onto a large shell-isolated gold core, which eliminates photocatalytic side reactions.

Heterogeneous catalysis with gold nanoparticles (Au NPs) has attracted considerable attention in the past two decades.[1] Although gold is the noblest of all the metals,[2] small Au NPs as catalysts have shown high selectivity and stability,[3] and more importantly, they are active even under mild conditions such as ambient temperature or less.[4] This is highly relevant for applications in areas such as pollution control and fuel cell systems.[5] Today, catalysis by Au NPs is an expanding area, and a large number of new catalytic systems for various reactions are now being explored.[6] However, label-free monitoring of heterogeneously catalyzed reactions by Au catalysts remains challenging at present for the following reasons: (1) complex heterogeneous reaction systems comprise the solid catalyst and the liquid/gas reaction solution; (2) chemical transformations are confined to the solution−catalyst interface; and (3) unstable reaction intermediates on the catalytic surface are difficult to separate and purify.

Absorption spectroscopies using infrared,[7] UV−vis,[8] and X-ray radiation[9] are candidate techniques for in situ study of Au-catalyzed reactions. However, absorption spectroscopy is not surface-selective and therefore suffers from the three limitations mentioned above. Additionally, infrared spectroscopy on aqueous systems is complicated by the strong water absorption. UV−vis absorption spectroscopy provides only very limited chemical information, while X-ray absorption spectroscopy can only characterize the solid catalyst. Surface-enhanced Raman scattering (SERS) combines the advantages of high chemical specificity[10] (vibrational Raman scattering), high sensitivity[11] (electromagnetic and chemical enhancement), and surface selectivity (near-field enhancement).[12] SERS therefore formally fulfills all criteria for label-free monitoring of molecular transformations in heterogeneous catalysis. On the other hand, Au NPs are widely used in SERS. Therefore, the question arises why SERS has not been used so far for label-free monitoring of reactions catalyzed by small Au NPs. Let us first assume that the same type of Au NPs exhibits both catalytic and SERS activity. In this hypothetical case, monitoring Au NP-catalyzed reactions by SERS would be very simple. Unfortunately, this is not the case in reality since the physicochemical properties of Au NPs are strongly size-dependent. Generally, Au NPs with a diameter of less than 10 nm exhibit catalytic activity,[4c,5c,13] but they cannot be used for efficient generation of SERS due to their very small scattering cross sections; typically only Au NPs larger than 20 nm have sufficient plasmonic activity and provide the required SERS enhancement.[14] However, these large, SERS-active Au NPs are not catalytically active anymore. The central dilemma is therefore that neither the small nor the large Au NPs alone exhibit both desired properties: catalytic and SERS activity.

Here, we demonstrate a rational chemical approach for integrating catalytically active small Au NPs with SERS-active large Au NPs into a single bifunctional metal superstructure. NP superstructures, produced either by the use of oligonucleotides/DNA[15] or by electrostatic attraction between NPs with opposite charges,[16] are of great interest due to their strong plasmonic activity. In this work, strong covalent Au−S bonds are used to construct Au NP superstructures to ensure their stability under real chemical reaction conditions. The Au core is encapsulated with a thin silica shell according to the concept of shell-isolated nanoparticle-enhanced Raman spectroscopy (SHINERS).[17] The thin silica coating around the large Au core has no pinhole and isolates the large Au core from direct contact with chemical species involved in the reaction. In a proof-of-concept study, we employ these rationally designed plasmonic superstructures for direct and label-free monitoring of the Au-catalyzed reduction of 4-nitrothiophenol (4-NTP) to the corresponding aniline derivative (4-ATP). This reaction was chosen as a model system because 4-NTP and 4-ATP are involved in several reactions: metal-catalyzed hydrogenation and surface plasmon resonance (SPR)-induced, photocatalyzed oxidation/reduction. These reactions and related molecules have been studied intensively in the past few years, and there is still an ongoing debate about the underlying reaction mechanisms, in particular the role of photocatalysis.[18−20] In the present study on this model reaction, photocatalysis and reagent-induced catalysis are disentangled: the ultrathin inert shell on the SERS-active core eliminates photocatalytic side reactions by spatially separating core and satellites.

Scheme 1 shows the synthesis of bifunctional plasmonic superstructures for integrated SERS monitoring of chemical reactions catalyzed by the small Au NP satellites. First, SERS-active Au NPs with a diameter of 80 nm are modified with (3-mercaptopropyl)trimethoxysilane (MPTMS). The modified

Received: September 12, 2012
Published: November 27, 2012

dx.doi.org/10.1021/ja309074a | J. Am. Chem. Soc. 2013, 135, 1657−1660

Scheme 1. Synthesis of Bifunctional 3D Au Superstructures

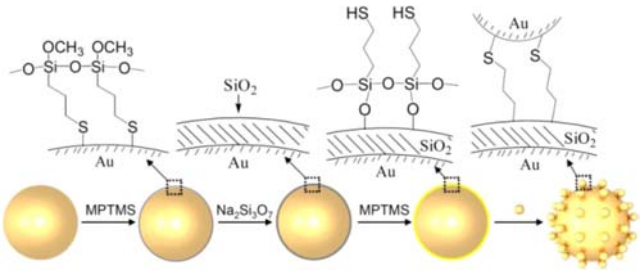

core particles are incubated with sodium silicate to form a thin inert silica shell coating around the Au core. The obtained silica-encapsulated NPs are then incubated again with MPTMS to functionalize their surface with thiol groups. Small Au NPs are subsequently mixed with the thiol-functionalized large NPs and captured by the thiol groups. Further experimental details are given in the Supporting Information.

Self-assembly of the small Au satellites onto the large Au core leads to a strong plasmonic coupling, as experimentally documented by a strong red shift of the plasmon peak upon self-assembly (Figure 1a). The plasmon peak of the single 5 and

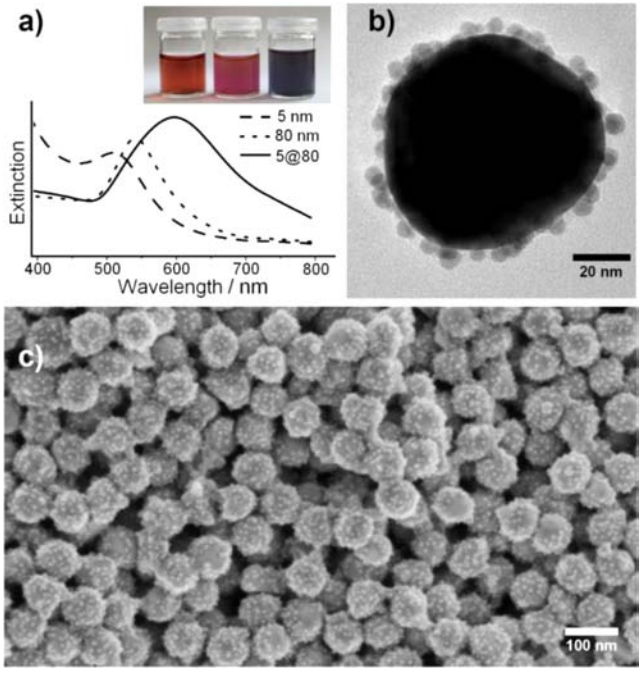

Figure 1. (a) Extinction spectra of 5 nm Au NPs, 80 nm Au NPs, and the 5 nm@80 nm Au superstructures. (b) TEM image of a single superstructure. (c) SEM image of an ensemble.

80 nm quasi-spherical Au NPs is at 516 and 547 nm, respectively, while the assemblies exhibit a red-shifted plasmon peak at 603 nm (Figure 1a). The transmission electron microscopy (TEM) image in Figure 1b indicates that indeed core/satellites superstructures have formed. The distance between the satellite Au NPs and the large Au core surface is about 1.5 nm (Figure S1), which is very favorable for strong plasmonic coupling and the generation of enhanced electric fields upon light irradiation. Free small Au NPs in the suspension, which are not bound on the core particle surface, are carefully removed by centrifugation. After washing several times with water, the 3D superstructures are obtained in large yields (Figure 1c).

Silica-encapsulated Au NPs with shell thicknesses of about 1.5, 10, and 20 nm are synthesized to investigate the influence of the silica shell on the SERS activity of the resulting Au superstructures (Figure S2). 4-NTP is used as the Raman reporter. The shell-isolated 80 nm Au NPs with a 1.5 nm ultrathin silica shell provide the strongest SERS enhancement. Due to the isolation of the Au core by the silica shell, their SERS spectrum is slightly different from that of 4-NTP chemisorbed on bare 80 nm Au NPs, i.e., without silica encapsulation. Specifically, the Raman band due to the symmetric NO_2 stretching vibration occurs at 1334 cm^{-1} in the SHINERS spectrum and at 1346 cm^{-1} in the bare Au NP-enhanced spectrum (Figure S3). The former is consistent with the peak position in the normal Raman spectrum of solid 4-NTP, demonstrating that the Au surface is completely covered by the inert silica shell[17] and direct contact between 4-NTP molecules and the Au surface has been blocked.

Small Au NPs with a diameter of about 5 nm are assembled on the shell-isolated 80 nm large Au cores (Figure S4). Raman reporter molecules (4-NTP) are added to the suspension of the Au superstructures to bind on the surface of the small bare Au NPs and form a self-assembled monolayer (SAM). The SERS intensity of 4-NTP is strongly distance-dependent (thickness of the silica shell). The superstructures with an ultrathin silica shell exhibit the highest SERS enhancement. Matching between the plasmon peak of the superstructure (603 nm, Figure 1a) and the excitation wavelength (632.8 nm) further enhances the SERS signal in addition to the strong plamonic coupling between the 5 nm Au satellites and the 80 nm Au core. Although the original shell-isolated NPs with 10 and 20 nm silica shells are themselves not SERS-active (Figure S3), their corresponding superstructures still have a low SERS activity due to the plasmonic coupling between the small satellites and the large Au core. As expected, the superstructures prepared by using shell-isolated NPs with a 10 nm silica shell have a higher SERS activity than those prepared with a 20 nm silica shell because of the distance-dependent plamonic coupling between the large core and the small satellites. We simulated the incident electric field amplitude $|E|$ upon resonant plasmon excitation of the assemblies containing 1.5, 10, and 20 nm silica shells using finite element method (FEM) (Figure S5). The SERS enhancement factor can be compared simply by the fourth power of $|E|$ as an approximation for the electromagnetic enhancement in SHINERS. The calculated maximum $|E|^4$ values at the hot spots of these superstructures are 1.86×10^5, 2.14×10^4, and 7.72×10^3, respectively, which correlate reasonably well with the experimental SERS results (Figure S4d).

Gold superstructures with small satellites on the surface of the ultrathin shell-coated 80 nm Au cores are used for SERS monitoring of the Au-catalyzed reduction of 4-NTP in colloidal suspension. The 4-NTP educt molecules are incubated together with the assemblies and form a dense SAM on the surface of the Au satellites. The catalytic reduction is initiated by adding sodium borohydride solution to the colloidal suspension. Au is a mild catalyst which allows for slow catalytic reactions. Therefore, kinetic in situ monitoring of the reaction is possible by collecting the SERS signal directly from the colloidal suspension at different reaction times. It is important to mention that both the ultrathin silica shell and the small satellites covalently assembled on the silica surface are stable during the catalytic reaction (Figure S6). The spectrum of the final product obtained from the catalytic reaction (Figure S7) shows the same spectral features as the SERS reference spectrum of 4-ATP. We propose that the reaction is catalyzed via electron transfer between the catalyti-

dx.doi.org/10.1021/ja309074a | J. Am. Chem. Soc. 2013, 135, 1657−1660

cally active Au surface and the nitro group through the molecule because direct contact of the nitro group to the Au surface is unlikely in the densely packed SAM. In contrast, large Au cores without small Au satellites cannot catalyze the reaction of 4-NTP to 4-ATP (Figure S8). The characteristic SERS spectra of the educt (4-NTP) and product (4-ATP) molecules are distinct from each other. Quantitative information on the relative concentration of the two components is extracted by comparing the intensities of the characteristic bands at 1569 and 1591 cm^{-1} (Figure 2a), which are due to phenyl ring modes of 4-NTP and 4-ATP, respectively. Since the Raman scattering cross section and the SERS response of 4-NTP and 4-ATP are different, the intensities of the two bands obtained under the same experimental condition are compared (Figure S9), and the relative concentrations of the two components in the mixed SAM are calculated using the corrected intensity of the corresponding bands. Figure 2b shows the changes in relative concentrations as a function of reaction time (black points).

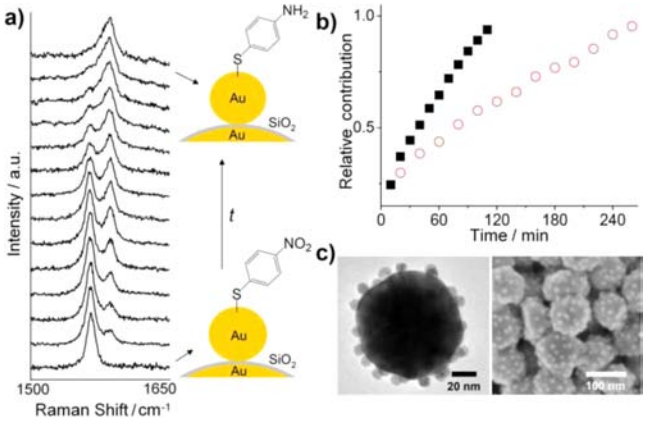

Figure 2. (a) SERS spectra from the reaction suspension collected at different reaction times. (b) Relative contributions of 4-ATP on the surface of 5 nm (black points) and 10 nm (red points) satellites as a function of reaction time. (c) TEM (left) and SEM (right) images of Au superstructures with 10 nm Au satellites assembled onto a 80 nm Au core isolated by an ultrathin silica shell.

Since the catalytic activity of metal NPs is size-dependent, we wanted to test experimentally whether the reaction rate of this Au-catalyzed reaction decreases with increasing size of the Au satellites on the surface of the shell-isolated Au core. We prepared Au superstructures with 10 nm Au satellites (instead of 5 nm Au NPs used in the standard protocol) assembled onto the shell-isolated Au cores (Figure 2c). In situ kinetic monitoring of the catalytic reaction was carried out at the same reaction conditions used for the 5 nm Au NP-catalyzed reaction (Figure S10). As expected, the reaction was retarded by using 10 nm Au NPs as satellites (Figure 2b, red points) due to the size-dependent catalytic activity of small Au NPs. Differences in the available catalytically active Au surface due to the different sizes of the satellites should not influence the reaction rate because adsorption-dependent processes on the superstructure are negligible due to the presence of a SAM; i.e., the accessible surface of the satellites is completely covered by of 4-NTP educt molecules.

In situ SERS kinetic monitoring can also provide insight into the reaction mechanisms of heterogeneously catalyzed reactions. The SERS spectra (Figure 2a) indicate that 4-NTP molecules are—given the limited time resolution of our experiment—converted directly into their corresponding aniline derivate 4-ATP. We performed two control experiments in order to investigate the role of the very thin silica shell, which isolates the 80 nm Au core from the environment (Figure 3a, right bottom),

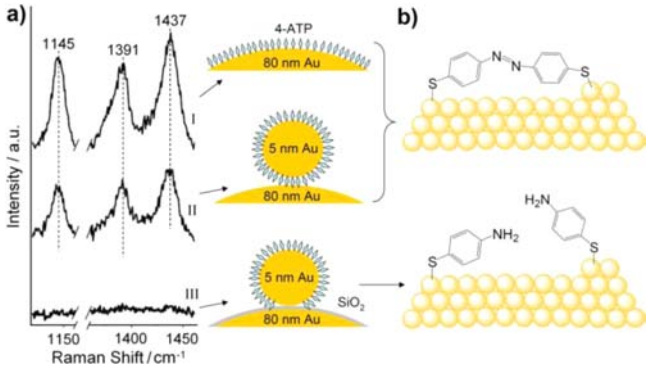

Figure 3. (a) SERS spectra collected from 4-ATP on bare 80 nm Au NPs (spectrum I), mixture of bare 80 nm Au NPs and 4-ATP covered 5 nm Au NPs (spectrum II), and Au superstructures with 5 nm Au satellites on top of silica shell-isolated 80 nm Au core (spectrum III). (b) Schematic of 4,4′-DMAB and 4-ATP on the Au surface.

on the corresponding SERS spectra: (1) 80 nm Au NPs with a SAM of 4-ATP (Figure 3a, right top) and (2) a mixture of bare 80 nm Au NPs and 5 nm Au NPs with a SAM of 4-ATP (Figure 3a, right middle). In both control experiments, vibrational Raman bands of 4,4′-dimercaptoazobenzene (4,4′-DMAB) at 1145, 1391, and 1437 cm^{-1} were detected (spectra I and II in Figure 3a). Interestingly, these three Raman bands did not appear in the SERS spectrum of the 4-ATP-coated assemblies on the shell-isolated Au cores (Figure 3a left, spectrum III), indicating that 4,4′-DMAB can be generated from 4-ATP only when the 4-ATP molecules have direct contact with the 80 nm Au core. This result is consistent with all the previous studies, in which these three bands of 4,4′-DMAB (at 1145, 1391, and 1437 cm^{-1}) were detected in cases where 4-ATP was directly exposed to a bare metal surface with strong plasmonic/SERS activity.[19] We hypothesize that plasmon-driven metal-to-molecule charge transfer facilitates the photocatalyzed conversion from 4-ATP to 4,4′-DMAB.

Gaining mechanistic insights into Au NP-catalyzed reactions at the molecular level requires noninvasive analysis. Although SERS has long been regarded as a nondestructive analytical method, in certain circumstances the use of bare, plasmonically active metal NPs can induce unwanted photocatalytic side reactions. In our metal superstructure, the inert silica shell between the central Au core and the small Au satellites prevents the 4-ATP molecules from direct contact with the metal surface of the core and enables SHINERS of Au NP-catalyzed reactions. Isolation of SERS substrates is crucial for in situ studies of catalytic reactions since different, in particular wrong conclusions will be drawn if the SERS-active metal surface is itself involved in the reaction. For example, in the catalytic reduction of 4-NTP by using Pt as catalyst, 4,4′-DMAB was detected when the 4-NTP molecules were not completely reduced because the SERS-active Au surface was accessible.[20] It is possible that 4,4′-DMAB was also generated in the Au-catalyzed reaction but was reduced immediately to 4-ATP by the reducing agent $NaBH_4$. We have tested for this option in an additional control experiment; 4,4′-DMAB was not observed when the educt (4-NTP) molecules were partially reduced by using an insufficient amount of

dx.doi.org/10.1021/ja309074a | J. Am. Chem. Soc. 2013, 135, 1657−1660

reducing agent (Figure S11). Therefore, in the Au-catalyzed reaction on the surface of the Au satellites in the assembly superstructure, 4-NTP is directly reduced to 4-ATP without a 4,4′-DMAB intermediate or side product. It is important to mention again that the inert ultrathin silica shell isolates the large Au core and thereby prevents its interaction with actual catalytic systems, e.g., avoiding the unwanted photoconversion of 4-ATP to 4,4′-DMAB.

In conclusion, we have rationally designed and synthesized 3D Au superstructures comprising a silica shell-isolated Au NP core and many catalytically active small Au satellites assembled on top of the silica shell for in situ monitoring of Au-catalyzed reactions. When an ultrathin silica shell (∼1.5 nm) was employed, the strong covalent Au−S bond captured the small Au NPs inside the local SPR field of the SERS-active core, and the chemical species on the small Au NP surface could therefore experience sufficient SERS enhancement. Moreover, the inert ultrathin silica shell on the Au core protects the metal surface from direct contact with the chemical species involved in the catalytic reaction and eliminates unwanted photocatalytic side reactions. Thus, the catalytic activity of the small Au satellite NPs and the mechanism of the Au NP-catalyzed, reagent-induced reaction can be investigated in situ and noninvasively via SERS. The presented approach is currently limited to molecular species containing a surface-seeking group in order to experience the necessary SERS enhancement. Capturing and enriching reactants on the surface of SERS substrates are promising methods for SERS monitoring of molecules without a surface-seeking group,[21] which have the potential to significantly expand the range of applications using the presented bifunctional Au superstructure.

■ ASSOCIATED CONTENT

Supporting Information

Experimental details, TEM/HR-TEM images, FEM simulations, and SERS spectra. This material is available free of charge via the Internet at http://pubs.acs.org.

■ AUTHOR INFORMATION

Corresponding Author

sebastian.schluecker@uos.de

Notes

The authors declare no competing financial interest.

■ ACKNOWLEDGMENTS

This work was supported by the Alexander von Humboldt Foundation. Technical support with HRTEM by Dr. K. Kömpe is acknowledged.

■ REFERENCES

(1) (a) Bond, G. C.; Louis, C.; Thompson, D. T. *Catalysis by Gold*; Imperial College Press: London, 2006. (b) Daniel, M. C.; Astruc, D. *Chem. Rev.* **2004**, *104*, 293.

(2) Hammer, B.; Norskov, J. K. *Nature* **1995**, *376*, 238.

(3) (a) Zope, B. N.; Hibbits, D. D.; Neurock, M.; Davis, R. J. *Science* **2010**, *330*, 74. (b) Thielecke, N.; Vorlop, K. D.; Prüsse, U. *Catal. Today* **2007**, *122*, 266.

(4) (a) Haruta, M.; Kobayashi, T.; Sano, H.; Yamada, N. *Chem. Lett.* **1987**, *16*, 405. (b) Haruta, M.; Yamada, N.; Kobayashi, T.; Iijima, S. *J. Catal.* **1989**, *115*, 301. (c) Valden, M.; Lai, X.; Goodman, D. W. *Science* **1998**, *281*, 1647. (d) Hughes, M. D.; Xu, Y. J.; Jenkins, P.; McMorn, P.; Landon, P.; Enache, D. I.; Carley, A. F.; Attard, G. A.; Hutchings, G. J.; King, F.; Stitt, E. H.; Johnston, P.; Griffin, K.; Kiely, C. J. *Nature* **2005**, *437*, 1132.

(5) (a) Fang, Y. L.; Heck, K. N.; Alvarez, P. J. J.; Wong, M. S. *ACS Catal.* **2011**, *1*, 128. (b) Corti, C. W.; Holliday, R. J.; Thompson, D. T. *Top. Catal.* **2007**, *44*, 331. (c) Thompson, D. T. *Nano Today* **2007**, *2*, 40.

(6) (a) Murdoch, M.; Waterhouse, G. I. N.; Nadeem, M. A.; Metson, J. B.; Keane, M. A.; Howe, R. F.; Llorca, J.; Idriss, H. *Nature Chem.* **2011**, *3*, 489. (b) Zhong, D. Y.; Franke, J. H.; Podiyanachari, S. K.; Blömker, T.; Zhang, H. M.; Kehr, G.; Erker, G.; Fuchs, H.; Chi, L. F. *Science* **2011**, *334*, 213.

(7) (a) Daniells, S. T.; Overweg, A. R.; Makkee, M.; Moulijn, J. A. *J. Catal.* **2005**, *230*, 52. (b) Shinizu, K.; Miyamoto, Y.; Kawasaki, T.; Tanji, T.; Tai, Y.; Satsuma, A. *J. Phys. Chem. C* **2009**, 17803. (c) Richner, G.; van Bokhoven, J. A.; Neuhold, Y. M.; Makosch, M.; Hungerbühler, K. *Phys. Chem. Chem. Phys.* **2011**, *13*, 12463.

(8) Chowdhury, B.; Bravo-Suarez, J. J.; Minura, N.; Lu, J. Q.; Bando, K. K.; Tsubota, S.; Haruta, M. *J. Phys. Chem. B* **2006**, *110*, 22995.

(9) Nijhuis, T. A.; Sacaliuc, E.; Beale, A. M.; van der Eerden, A. M. J.; Schouten, J. C.; Weckhuysen, B. M. *J. Catal.* **2008**, *258*, 256.

(10) (a) Cortes, E.; Etchegoin, P. G.; Ru, E. C. L.; Fainstein, A.; Vela, M. E.; Salvarezza, R. C. *J. Am. Chem. Soc.* **2010**, *132*, 18034. (b) Cao, Y. W. C.; Jin, R. C.; Mirkin, C. A. *Science* **2002**, *297*, 1536.

(11) (a) Nie, S. M.; Emory, S. R. *Science* **1997**, *275*, 1102. (b) Kneipp, K.; Wang, Y.; Kneipp, H.; Perelman, L. T.; Itzkan, I.; Dasari, R. R.; Feld, M. S. *Phys. Rev. Lett.* **1997**, *78*, 1667.

(12) Heck, K. N.; Janesko, B. G.; Scuseria, G. E.; Halas, N. J.; Wong, M. S. *J. Am. Chem. Soc.* **2008**, *130*, 16592.

(13) (a) Sinha, A. K.; Seelan, S.; Tsubota, S.; Haruta, M. *Top. Catal.* **2004**, *29*, 95. (b) Campbell, C. T. *Science* **2004**, *306*, 234.

(14) (a) Krug, J. T.; Wang, G. D.; Emory, S. R.; Nie, S. M. *J. Am. Chem. Soc.* **1999**, *121*, 9208. (b) Bell, S. E. J.; McCourt, M. R. *Phys. Chem. Chem. Phys.* **2009**, *11*, 7455.

(15) (a) Xu, X. Y.; Rosi, N. L.; Wang, Y. H.; Huo, F. W.; Mirkin, C. A. *J. Am. Chem. Soc.* **2006**, *128*, 9286. (b) Sebba, D. S.; Mock, J. J.; Smith, D. R.; LaBean, T. H.; Lazarides, A. A. *Nano Lett.* **2008**, *8*, 1803. (c) Xu, L. G.; Kuang, H.; Xu, C. L.; Ma, W.; Wang, L. B.; Kotov, N. A. *J. Am. Chem. Soc.* **2012**, *134*, 1699.

(16) (a) Gellner, M.; Steinigeweg, D.; Ichilmann, S.; Salehi, M.; Schütz, M.; Kömpe, K.; Haase, M.; Schlücker, S. *Small* **2011**, *7*, 3445. (b) Gandra, N.; Abbas, A.; Tian, L. M.; Singamaneni, S. *Nano Lett.* **2012**, *12*, 2645.

(17) Li, J. F.; Huang, Y. F.; Ding, Y.; Yang, Z. L.; Li, S. B.; Zhou, X. S.; Fan, F. R.; Zhang, W.; Zhou, Z. Y.; Wu, D. Y.; Ren, B.; Wang, Z. L.; Tian, Z. Q. *Nature* **2010**, *464*, 392.

(18) Joseph, V.; Engelbrekt, C.; Zhang, J. D.; Gernert, U.; Ulstrup, J.; Kneipp, J. *Angew. Chem., Int. Ed.* **2012**, *51*, 7592.

(19) (a) Kim, K.; Lee, S. J.; Kim, K. L. *J. Phys. Chem. B* **2004**, *108*, 16208. (b) Zhou, Q.; Li, X. W.; Fan, Q.; Zhang, X. X.; Zheng, J. W. *Angew. Chem., Int. Ed.* **2006**, *45*, 3970. (c) Fang, Y. R.; Li, Y. Z.; Xu, H. X.; Sun, M. T. *Langmuir* **2010**, *26*, 7737. (d) Huang, Y .F.; Zhu, H .P.; Liu, G. K.; Wu, D. Y.; Ren, B.; Tian, Z. Q. *J. Am. Chem. Soc.* **2010**, *132*, 9244. (e) Kim, K.; Shin, D.; Kim, K. L.; Shin, K. S. *Phys. Chem. Chem. Phys.* **2012**, *14*, 4095. (f) Huang, Y. F.; Wu, D. Y.; Zhu, H. P.; Zhao, L. B.; Liu, G. K.; Ren, B.; Tian, Z. Q. *Phys. Chem. Chem. Phys.* **2012**, *14*, 8485.

(20) Xie, W.; Herrmann, C.; Kömpe, K.; Haase, M.; Schlücker, S. *J. Am. Chem. Soc.* **2011**, *133*, 10302.

(21) (a) Alvarez-Puebla, R. A.; Contreras-Caceres, R.; Pastoriza-Santos, I.; Perez-Juste, J.; Liz-Marzan, L. M. *Angew. Chem., Int. Ed.* **2009**, *48*, 138. (b) Shafer-Peltier, K. E.; Haynes, C. L.; Glucksberg, M. R.; Van Duyne, R. P. *J. Am. Chem. Soc.* **2003**, *125*, 588.